NASA TECHNICAL MEMORANDUM

UB
NASA TM X-1148

LATERAL AERODYNAMIC CHARACTERISTICS OF A CONCEPTUAL HORIZONTAL-TAKE-OFF REUSABLE LAUNCH VEHICLE FROM MACH 3 TO 6

by John D. Norris and John P. Decker

Langley Research Center
Langley Station, Hampton, Va.

NATIONAL AERONAUTICS AND SPACE ADMINISTRATION • WASHINGTON, D. C. • SEPTEMBER 1965

[redacted] NASA TM X-1148

LATERAL AERODYNAMIC CHARACTERISTICS OF A CONCEPTUAL HORIZONTAL-TAKE-OFF REUSABLE LAUNCH VEHICLE FROM MACH 3 TO 6

By John D. Norris and John P. Decker

Langley Research Center
Langley Station, Hampton, Va.

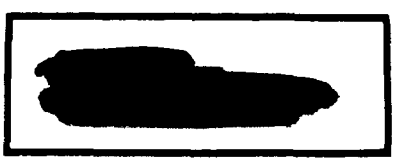

[redacted]

NATIONAL AERONAUTICS AND SPACE ADMINISTRATION

[redacted]

[redacted]SIFIED

LATERAL AERODYNAMIC CHARACTERISTICS OF A CONCEPTUAL HORIZONTAL-TAKE-OFF REUSABLE LAUNCH VEHICLE FROM MACH 3 TO 6*

By John D. Norris and John P. Decker
Langley Research Center

SUMMARY

20079

A wind-tunnel investigation of the lateral aerodynamic characteristics was made at supersonic and hypersonic speeds of an approximate 1/125-scale model of a conceptual multistage horizontal-take-off reusable launch vehicle. The model consisted of a winged reusable first stage with a canard, a winged reusable second stage, and a winged third-stage reusable spacecraft with an expendable maneuver propulsion package. The two upper stages were arranged in tandem, and this combination was placed parallel to the first-stage reusable booster. The model was tested at Mach numbers of 3.0, 4.5, and 6.0, at angles of attack from about -4° to 19°, and generally at angles of sideslip of 0° and 5°. The test Reynolds number per foot (per 30.5 cm) varied from approximately 1.0×10^6 to 2.1×10^6.

The complete first stage had positive effective dihedral throughout the positive angle-of-attack range at a Mach number of 3.0. Increasing Mach number caused a decrease in effective dihedral, and at a Mach number of 6.0 the complete first stage exhibited positive effective dihedral only above an angle of attack of 7°. The complete first stage was directionally unstable about the selected moment-reference center except for small angles of attack at a Mach number of 3.0 where it was approximately neutrally stable. The addition of the complete upper stages to the first stage caused a reduction in positive effective dihedral and directional stability. The complete launch vehicle was directionally unstable throughout the test Mach number and angle-of-attack range. Removal of the propulsion package from the upper-stage configuration had a favorable influence on the directional stability of the launch vehicle.

INTRODUCTION

A research program is being conducted at the NASA Langley Research Center to study some of the aerodynamic problems associated with launch vehicles incorporating reusable components. Results of investigations on models of horizontal

---

*[redacted]

take-off and reusable launch vehicles are given in references 1 to 7. The present tests were conducted to determine the lateral aerodynamic characteristics of a conceptual horizontal-take-off reusable launch vehicle at Mach numbers from 3.0 to 6.0. Longitudinal aerodynamic characteristics and longitudinal aerodynamic separation characteristics for this model at the same Mach numbers as those for the present investigation are reported in references 1 and 2, respectively. Both lateral and longitudinal aerodynamic characteristics at transonic and low supersonic speeds are reported in references 3 and 4, respectively.

The complete launch vehicle consisted of a winged reusable first stage with a canard, a winged reusable second stage, and a third-stage winged reusable spacecraft with an expendable propulsion package for in-orbit maneuvering. The upper stages were arranged in tandem, and this combination was placed parallel to the first stage. The first-stage canard was incorporated primarily to satisfy the control requirements of the first stage during its reentry phase back into the sensible atmosphere.

All stages of the vehicle were conceived to employ rocket engines using liquid oxygen and hydrogen propellants during boost. The first stage was assumed to utilize turbojet engines as its return propulsion system during subsonic flight while the second and spacecraft stages were considered to be glide return vehicles.

The launch vehicle was designed to place a maximum of 20 000 pounds (9080 kg) of spacecraft into a low earth orbit. The vehicle was assumed to be rocket powered and to perform a rapid pull-up, keeping the total acceleration between 2.5g and 3.0g, in order to enter a ballistic trajectory and to minimize the gravity losses. Stage separation was estimated to occur at a speed of 6500 fps (1.9812 km/s) at an altitude of about 230 000 feet (70.104 km), and the take-off wing loading was assumed to be 120 lb/sq ft ($5.7456\ N/m^2$), based on total wing area.

Tests were conducted on a 1/125-scale model in the 2-foot hypersonic facility at the Langley Research Center to investigate the lateral aerodynamic characteristics at Mach numbers of 3.0, 4.5, and 6.0, at angles of attack from approximately -4° to 19°, and generally at angles of sideslip of 0° and 5°. The Reynolds numbers per foot (per 30.5 cm) over the Mach number range varied from approximately 1.0×10^6 to 2.1×10^6.

SYMBOLS

The units used for the physical quantities in this paper are given in both U.S. Customary Units and the International System of Units (SI). Factors relating the two systems are given in reference 8 and those used in the present study are presented in the appendix.

Lateral and directional force and moment coefficients are referred to the body axes. The moment reference center is located at 15 percent of the mean aerodynamic chord of the first-stage wing, and was 7.480 inches (19.00 cm)

forward of the model base in the stage separation plane. (See fig. 1(a).) All aerodynamic coefficients are based on the geometry of the wing of the first-stage reusable booster.

C_l rolling-moment coefficient, $\frac{\text{Rolling moment}}{qSb}$

C_n yawing-moment coefficient, $\frac{\text{Yawing moment}}{qSb}$

C_Y side-force coefficient, $\frac{\text{Side force}}{qS}$

C_{l_β} effective-dihedral parameter, $\frac{\Delta C_l}{\Delta \beta}$, per deg

C_{n_β} directional-stability parameter, $\frac{\Delta C_n}{\Delta \beta}$, per deg

C_{Y_β} side-force parameter, $\frac{\Delta C_Y}{\Delta \beta}$, per deg

b reference wing span, 0.800 ft (0.2438 m)

c aerodynamic chord, ft (m)

$\bar{c}$ reference mean aerodynamic chord, based on total wing area, 0.733 ft (0.2234 m)

M free-stream Mach number

p_t total pressure, atm (N/m^2)

q free-stream dynamic pressure, lb/sq ft (N/m^2)

S reference wing area, 0.440 sq ft $(0.041\ m^2)$

T_t total temperature, $^\circ R$ $(^\circ K)$

α angle of attack (referred to stage-separation plane), deg

β angle of sideslip, deg

Component symbols:

B fuselage, first or second stage

W wing, first or second stage

C	canard
N	nacelles, first stage
F	vertical fins, first or second stage
M	maneuver propulsion package
S	spacecraft with mounting pad

DESCRIPTION OF MODEL

The complete launch vehicle and its components are shown in figure 1. The launch vehicle consisted of a winged reusable first stage with a canard, a winged reusable second stage, and a winged third-stage reusable spacecraft with an expendable space-maneuvering propulsion package. The two upper stages were arranged in tandem, and this combination was placed parallel to the first-stage reusable booster. Principal model dimensions are presented in table I, and photographs of the model are shown in figure 2.

First-Stage Reusable Booster

The first-stage reusable booster consisted of a semicylindrical fuselage with an ogival forebody, a delta canard, and a delta wing with trapezoidal vertical fins mounted outboard on nacelles. (See fig. 1(b).) The wing had 70° of leading-edge sweep and was a symmetrical wedge to the 40-percent chord station with a constant 0.05c maximum thickness rearward to the 0.85c station. A wedge or boattail on the lower surface of the wing extended from 0.85c to the wing trailing edge. (See fig. 1(c).) The first-stage wing was flat on the upper surface rearward of the 40-percent chord station to allow mating with the second-stage wing. The wing was set at an incidence angle of 0°. The requirement for a flat upper surface resulted in a wing dihedral angle of about $3\frac{1}{2}^{\circ}$. The exposed area of the canard was approximately 7 percent of the total first-stage wing area, and the distance between $0.25\bar{c}$ of the canard and $0.25\bar{c}$ of the first-stage wing was $1.4\bar{c}$ of the wing.

The first-stage vertical fins were located outboard at 2/3 of the wing semispan and the total fin area, which was equally distributed above and below the wing, was approximately 15 percent of the total wing area. The vertical fins had a panel aspect ratio of 1.15 and a taper ratio of 0.5. The nacelles were cylindrical with a parabolic nose and were considered to house the flyback engines which for these tests had plugged inlets. The nacelles formed the juncture between the first-stage wing and vertical fins.

Second-Stage Reusable Booster

The second-stage reusable booster consisted of a cylindrical fuselage and a trapezoidal wing with two outboard-mounted vertical fins located at 2/3 of the wing semispan. The fuselage incorporated a side fairing which extended vertically from the center line of the second-stage fuselage to the upper surface of the first-stage fuselage.

The second-stage wing thickness was chosen to achieve a total profile thickness of 0.065c (based on the chord of the first-stage wing) when the first- and second-stage wings were mated. The forward 0.40c of the upper surface of the second-stage wing formed a coplanar surface with the first-stage wing. A portion of the leading edge of this extension was removed to form a constant leading-edge radius on the second-stage wing identical to that of the first-stage wing. The purpose of this arrangement was to reduce the interference of the mated wings during launch. The second-stage vertical fins were similar to the first-stage vertical fins, but only the upper element was employed.

Orbital Stage

The orbital stage consisted of a spacecraft and a maneuver propulsion package. The spacecraft was a wing-body configuration with toed-in, wing-tip-mounted vertical fins. (See fig. 1(d).) The spacecraft wing was unsymmetrical with the camber adjacent to the spacecraft pad, and the span (including vertical fins) was approximately equal to the width of the first-stage fuselage. A pad was used to support the spacecraft on the launch vehicle. The maneuver propulsion package was an expendable rocket booster designed as a short cylinder with the same diameter as the second-stage fuselage and also incorporating the same type of side fairing as the second-stage fuselage. When the model was tested without the maneuver propulsion package, the spacecraft was moved rearward to connect directly with the second-stage fuselage. This configuration is considered to meet the requirement for missions not needing appreciable in-orbit maneuvering.

APPARATUS AND TESTS

The tests were conducted in the 2-foot hypersonic facility at the Langley Research Center (described in ref. 9) at nominal Mach numbers of 3.0, 4.5, and 6.0, at angles of attack from approximately -4° to 19°, and generally at angles of sideslip of 0° and 5°. The test Reynolds number per foot (per 30.5 cm) varied from approximately 1.0×10^6 to 2.1×10^6.

Static aerodynamic force and moment data were obtained by means of a six-component internally mounted strain-gage balance. All data were obtained with the model surface smooth, and, at the Reynolds numbers of these tests, laminar flow would be expected over almost the entire model. The angles of attack and sideslip were corrected for balance and sting deflection under load.

The average test conditions and Reynolds number variation during a typical launch trajectory for the complete vehicle and a typical flyback trajectory for the first stage are given in the following table:

M	β, deg	p_t		T_t		Reynolds number (based on overall length of vehicle) at -		
		atm	kN/m^2	^oR	^oK	Test	Launch	Flyback
3.0	0 and 5.30	1.0	101 325	560	311	4.2×10^6	7.0×10^6	31×10^6
4.5	0 and 5.15	1.5	151 988	760	422	2.0	2.4	25
6.0	0 and 5.10	3.4	344 505	760	422	2.2	1.6	9

It is seen from this table that the Reynolds numbers for the launch trajectory are in close agreement to the test Reynolds numbers, but the Reynolds numbers for the flyback trajectory of the first stage are considerably higher.

PRESENTATION OF RESULTS

The basic lateral aerodynamic characteristics are given in figures 3 to 5. Some results are summarized in figures 6 to 8. An outline of the contents of the data figures is as follows:

DISCUSSION OF RESULTS

Except where noted, the discussion indicates the important lateral aerodynamic characteristics of the complete first stage and the complete launch vehicle.

First-Stage Reusable Booster

Figure 3 shows that the basic lateral aerodynamic characteristics for the complete first stage are essentially linear with sideslip angle (at approximately $\alpha = 5^\circ$) between $\beta = -4^\circ$ and $+5^\circ$ and to have only small deviations from linearity for the extreme sideslip-angle range. Figure 6(a) shows that the complete first stage had positive effective dihedral $\left(-C_{l_\beta}\right)$ throughout the positive angle-of-attack range at $M = 3.0$. Increasing the Mach number caused some decrease in the positive effective dihedral, and at $M = 6.0$ the complete first stage exhibited positive effective dihedral only above $\alpha = 7^\circ$.

Figures 4 and 7 demonstrate the component effects on the first-stage reusable booster. The canard caused some increase in the positive effective dihedral but became less effective with increasing Mach number. Removal of the nacelles and fins caused little discernible change in C_{l_β}. This result is caused by the fins and nacelles being symmetrical, with their resultant center of pressure very near the vertical reference plane.

The complete first stage exhibited approximately neutral directional stability about the selected moment reference of $0.15\bar{c}$ at $M = 3.0$ for angles of attack less than 6°. (See fig. 6(b).) At higher angles of attack for $M = 3.0$ and throughout the angle-of-attack range at $M = 4.5$ and 6.0, the complete first stage was directionally unstable. The canard increased directional stability at the higher angles of attack at all Mach numbers. (See figs. 4 and 7.) Removal of the fins from the complete first stage caused the expected decrease in C_{n_β}. A first-order approximation of the effects of the fins on C_{Y_β} and C_{n_β} can be obtained by applying supersonic flat-plate theory $\left(C_{Y_\beta}/\text{rad} = \frac{4}{\sqrt{M^2 - 1}}\right)$ with the appropriate total fin area and moment arm.

Launch Vehicle

The addition of the complete upper stages to the complete first stage caused some reductions in positive effective dihedral at all test Mach numbers. (See fig. 6(a).) This result amounted to an equivalent reduction in effective dihedral of approximately 2° at $M = 3.0$ and approximately 1° at $M = 6.0$. Figure 6(a) also indicates that the complete launch vehicle had positive effective dihedral throughout the test Mach number range only above an angle-of-attack of about 8°. Removal of the maneuver propulsion package had little effect on C_{l_β} at all test Mach numbers. (See fig. 8.)

Figure 6(b) shows that the addition of the complete upper stages to the complete first stage caused destabilizing increments in directional stability at all test Mach numbers. These destabilizing increments are caused by unfavorable side force ahead of the moment-reference center and also a possible blanketing effect on the first-stage fins by the upper stages. At the highest test angles of attack, this destabilizing effect was not as pronounced as it

was at the lower angles of attack. The complete launch vehicle was directionally unstable at all test Mach numbers. Removal of the maneuver propulsion package (fig. 8) had a large favorable influence on stability resulting from the reduction of a sizable amount of side force on this component ahead of the moment reference center.

SUMMARY OF RESULTS

An investigation was made in a 2-foot hypersonic facility at the Langley Research Center of a multistage horizontal-take-off reusable launch vehicle. The lateral aerodynamic characteristics of the first-stage reusable booster and the complete launch vehicle with some stage and component effects were determined at Mach numbers of 3.0, 4.5, and 6.0, at angles of attack from about -4° to 19°, and generally at angles of sideslip of 0° and 5°. The test Reynolds number per foot (per 30.5 cm) varied from approximately 1.0×10^6 to 2.1×10^6. The principal results may be summarized as follows:

1. The complete first stage had positive effective dihedral throughout the positive angle-of-attack range at a Mach number of 3.0. Increasing Mach number caused a decrease in effective dihedral, and at a Mach number of 6.0 the complete first stage exhibited positive effective dihedral only above an angle of attack of 7°.

2. The complete first stage was directionally unstable about the selected moment-reference center except for small angles of attack at a Mach number of 3.0 where it was approximately neutrally stable.

3. The addition of the complete upper stages to the complete first stage caused a reduction in positive effective dihedral and directional stability at all test Mach numbers. The complete launch vehicle was directionally unstable throughout the test Mach number and angle-of-attack ranges.

4. Removal of the propulsion package from the upper-stage configuration had a favorable influence on the directional stability of the launch vehicle.

Langley Research Center,
National Aeronautics and Space Administration,
Langley Station, Hampton, Va., June 10, 1965.

APPENDIX

CONVERSION OF U.S. CUSTOMARY UNITS TO SI UNITS

Factors required for converting the U.S. Customary Units used herein to the International System of Units (SI) are given in the following table:

Physical quantity	U.S. Customary Unit	Conversion factor (*)	SI unit
Area	$in.^2$	0.000645	$meters^2$ (m^2)
	ft^2	0.0929	$meters^2$ (m^2)
Length	in.	0.0254	meters (m)
	ft	0.3048	meters (m)
Mass	lb	0.454	kilograms (kg)
Pressure	atm	101,325	$newtons/meter^2$ (N/m^2)
	psf	47.88026	$newtons/meter^2$ (N/m^2)
Temperature	^oR	5/9	degrees Kelvin (^oK)
Velocity	fps	0.3048	meters/second (m/s)

*Multiply value given in U.S. Customary Unit by conversion factor to obtain equivalent value in SI unit.

Prefixes to indicate multiples of units are as follows:

Prefix	Multiple
centi	10^{-2}
kilo	10^3

REFERENCES

1. Clark, Larry R.; and Decker, John P.: Longitudinal Aerodynamic Characteristics of a Model of a Horizontal-Take-Off Reusable Launch Vehicle at Mach Numbers From 3 to 6. NASA TM X-1030, 1964.

2. Decker, John P.; and Pierpont, P. Kenneth: Aerodynamic Separation Characteristics of a Conceptual Parallel-Staged Reusable Launch Vehicle at Mach 3 to 6. NASA TM X-1051, 1965.

3. Clark, Larry R.; and Pierpont, P. Kenneth: Transonic Characteristics of a Hydrogen-Fueled Multistage Horizontal-Take-Off Reusable Launch Vehicle. NASA TM X-1008, 1964.

4. Decker, John P.; and Clark, Larry R.: Static Aerodynamic Characteristics of a Model of a Horizontal-Take-Off Reusable Launch Vehicle at Mach Numbers 1.60, 2.16, and 2.86. NASA TM X-1097, 1965.

5. Clark, Larry R.; and Pierpont, P. Kenneth: Spacecraft and Stage-Geometry Effects on the Hypersonic Characteristics of a Horizontal-Take-Off Reusable Booster. NASA TM X-900, 1963.

6. Pierpont, P. Kenneth: Transonic Aerodynamic Characteristics of a Horizontal-Take-Off-and-Horizontal-Landing Recoverable-Booster Concept With Upper Stages Arranged in Parallel. NASA TM X-696, 1962.

7. Pierpont, P. Kenneth: Transonic Longitudinal and Lateral Aerodynamic Characteristics of a Preliminary Concept of a First-Stage Horizontal-Take-Off-and-Horizontal-Landing Recoverable Booster With a 70° Delta Wing. NASA TM X-691, 1962.

8. Mechtly, E. A.: The International System of Units - Physical Constants and Conversion Factors. NASA SP-7012, 1964.

9. Stokes, George M.: Description of a 2-Foot Hypersonic Facility at the Langley Research Center. NASA TN D-939, 1961.

TABLE I.- GEOMETRIC DESIGN CHARACTERISTICS OF MODEL

First stage -		
Fuselage:		
Length, in. (cm)	23.760	(60.35)
Equivalent base diameter, in. (cm)	2.304	(5.85)
Maximum height, in. (cm)	1.922	(4.88)
Nose radius, in. (cm)	0.096	(0.244)
Base area, sq in. (cm^2)	4.164	(26.86)
Wing:		
Total area, sq in. (cm^2)	63.360	(408.67)
Exposed area, sq in. (cm^2)	34.432	(222.09)
Span, in. (cm)	9.600	(24.38)
Root chord, in. (cm)	13.200	(33.53)
Maximum thickness, percent chord		3.500
Leading-edge sweep angle, deg		70
Leading-edge radius, in. (cm)	0.024	(0.061)
Mean aerodynamic chord, in. (cm)	8.800	(22.35)
Moment reference center, percent M.A.C.		15
Moment reference center, in. from base (cm from base)	7.480	(19.00)
Vertical fins:		
Area (exposed), sq in. (cm^2)	2.304	(14.86)
Height (exposed), in. (cm)	1.152	(2.93)
Root chord, in. (cm)	2.664	(6.77)
Tip chord, in. (cm)	1.332	(3.38)
Leading-edge sweep angle, deg		60
Trailing-edge sweep angle, deg		29.921
Leading-edge radius, in. (cm)	0.024	(0.061)
Wing nacelles:		
Length, in. (cm)	3.982	(10.11)
Maximum diameter, in. (cm)	0.576	(1.46)
Fineness ratio		6.910
Nose radius, in. (cm)	0.096	(0.244)
Canard:		
Total area, sq in. (cm^2)	12.804	(82.59)
Exposed area, sq in. (cm^2)	4.478	(28.88)
Span, in. (cm)	4.320	(10.97)
Root chord, in. (cm)	5.928	(15.06)
Tip chord, in. (cm)		0
Maximum thickness, percent chord		5
Leading-edge sweep angle, deg		70
Leading-edge radius, in. (cm)	0.024	(0.061)
Second stage -		
Fuselage:		
Length, in. (cm)	9.600	(24.38)
Equivalent base diameter, in. (cm)	1.368	(3.47)
Base area, sq in. (cm^2)	1.464	(9.44)

TABLE I.- GEOMETRIC DESIGN CHARACTERISTICS OF MODEL - Concluded

Wing:		
Total area, sq in. (cm^2)	27.072	(174.61)
Exposed area, sq in. (cm^2)	18.612	(120.05)
Span, in. (cm)	5.760	(14.63)
Root chord, in. (cm)	7.068	(17.95)
Tip chord, in. (cm)	2.311	(5.87)
Maximum thickness, percent chord		2.800
Leading-edge sweep angle, deg		58.753
Leading-edge radius, in. (cm)	0.024	(0.061)
Mean aerodynamic chord, in. (cm)	5.085	(12.92)
Moment reference center, in. from base (cm from base)	7.480	(19.00)
Vertical fins:		
Area (exposed), sq in. (cm^2)	2.276	(14.68)
Height, in. (cm)	1.249	(3.17)
Root chord, in. (cm)	2.580	(6.55)
Tip chord, in. (cm)	1.332	(3.38)
Leading-edge sweep angle, deg		60
Trailing-edge sweep angle, deg		29.921
Leading-edge radius, in. (cm)	0.024	(0.061)
Spacecraft -		
Fuselage:		
Length, including interstage, in. (cm)	6.048	(15.36)
Diameter, in. (cm)	0.672	(1.71)
Interstage base diameter, in. (cm)	1.280	(3.25)
Interstage taper, included angle, deg		35.200
Length of nose cone, in. (cm)	0.857	(2.176)
Nose cone included angle, deg		35
Nose radius, in. (cm)	0.096	(0.244)
Wing:		
Total area, sq in. (cm^2)	8.527	(55.00)
Exposed area, sq in. (cm^2)	5.347	(34.49)
Span in. (cm)	2.506	(6.37)
Root chord, in. (cm)	5.296	(13.45)
Tip chord, in. (cm)	1.589	(4.04)
Maximum thickness, percent chord		5
Leading-edge sweep angle, deg		72.500
Leading-edge radius, in. (cm)	0.024	(0.061)
Wing nose radius, in. (cm)	0.096	(0.244)
Vertical fins:		
Area, sq in. (cm^2)	0.866	(5.59)
Height, in. (cm)	0.858	(2.18)
Root chord, in. (cm)	1.589	(4.04)
Tip chord, in. (cm)	0.480	(1.22)
Maximum thickness, percent chord		5
Leading-edge sweep angle, deg		55
Leading-edge radius, in. (cm)	0.024	(0.061)
Lateral inclination angle, deg		3
Maneuver propulsion package:		
Length, in. (cm)	2.880	(7.32)
Equivalent circular diameter, in. (cm)	1.368	(3.47)

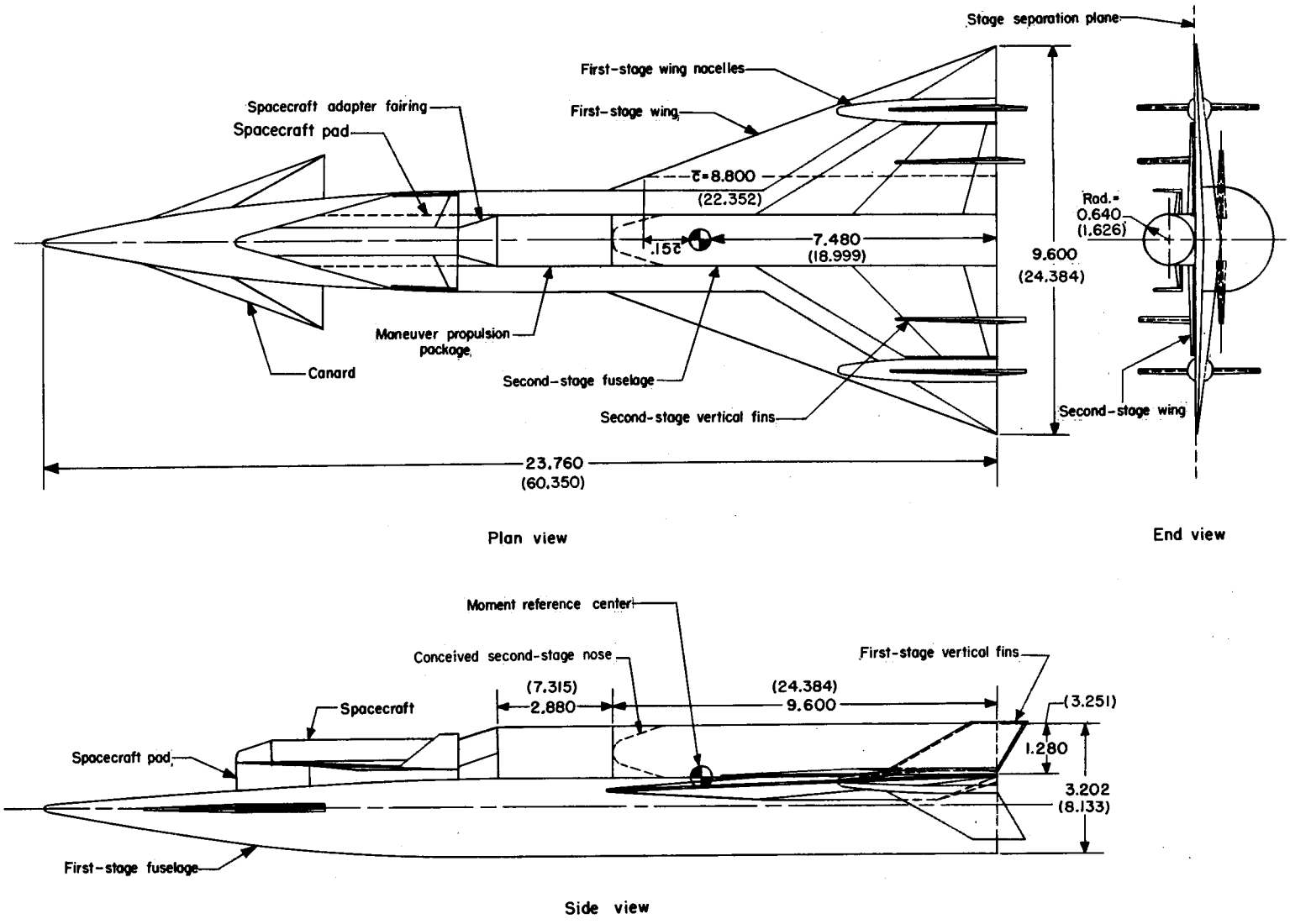

(a) General arrangement of launch vehicle.

Figure 1.- Arrangement and geometric details of a three-stage horizontal take-off reusable booster system. All linear design dimensions are in inches. (Parenthetical dimensions in centimeters.)

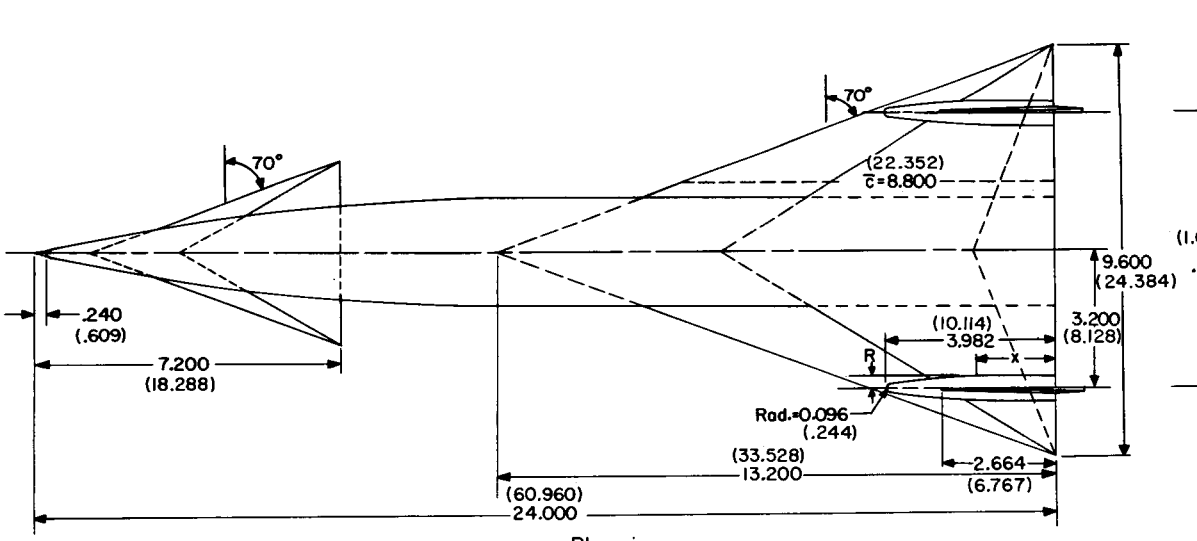

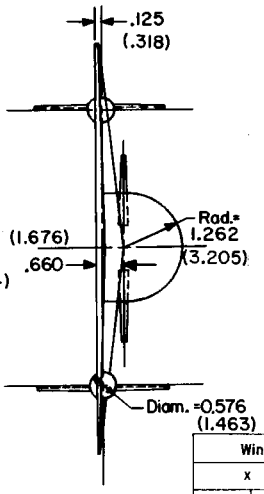

Wing pod coordinates			
x		r	
in.	cm	in.	cm
0	0	0.288	0.732
1.722	4.374	.288	.732
2.222	5.644	.278	.706
2.722	6.914	.247	.627
3.222	8.184	.196	.498

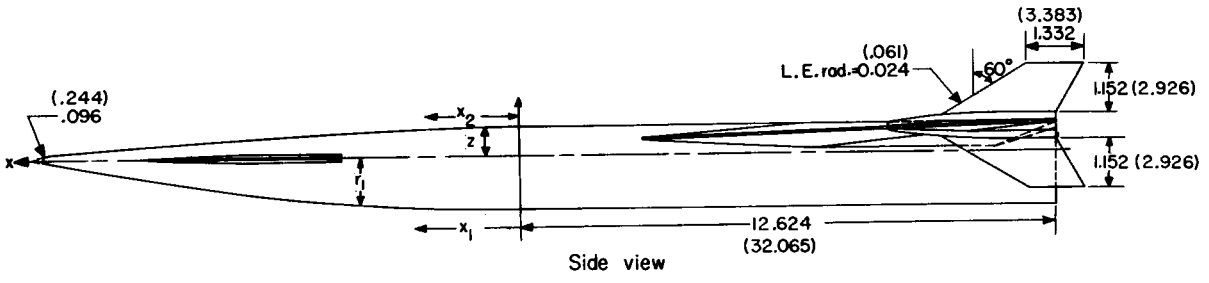

Fuselage coordinates							
x		r_1		x_2		z	
in.	cm	in.	cm	in.	cm	in.	cm
0	0	1.262	3.21	0	0	0.660	1.68
1.000	2.54	1.253	3.18	1.376	3.50	.618	1.57
1.999	5.08	1.223	3.11	2.376	6.04	.587	1.49
3.000	7.62	1.114	2.83	3.376	8.58	.553	1.40
4.000	10.16	1.106	2.81	4.376	11.16	.517	1.31
5.000	12.70	1.018	2.59	4.776	12.13	.479	1.22
6.000	15.24	.910	2.31	6.376	16.20	.438	1.11
7.000	17.78	.783	1.99	7.376	18.74	.391	.99
8.000	20.32	.636	1.62	8.376	21.28	.338	.86
9.000	22.86	.470	1.19	9.376	23.82	.277	.70
10.000	25.4	.284	.721	9.876	25.09	.239	.61
11.000	27.94	.079	.201	10.376	26.36	.195	.50
11.376	28.90	0	0	10.626	26.99	.169	.43
				10.876	27.63	.138	.35
				11.126	28.26	.098	.25
				11.376	28.90	0	0

(b) First-stage reusable booster.

Figure 1.- Continued.

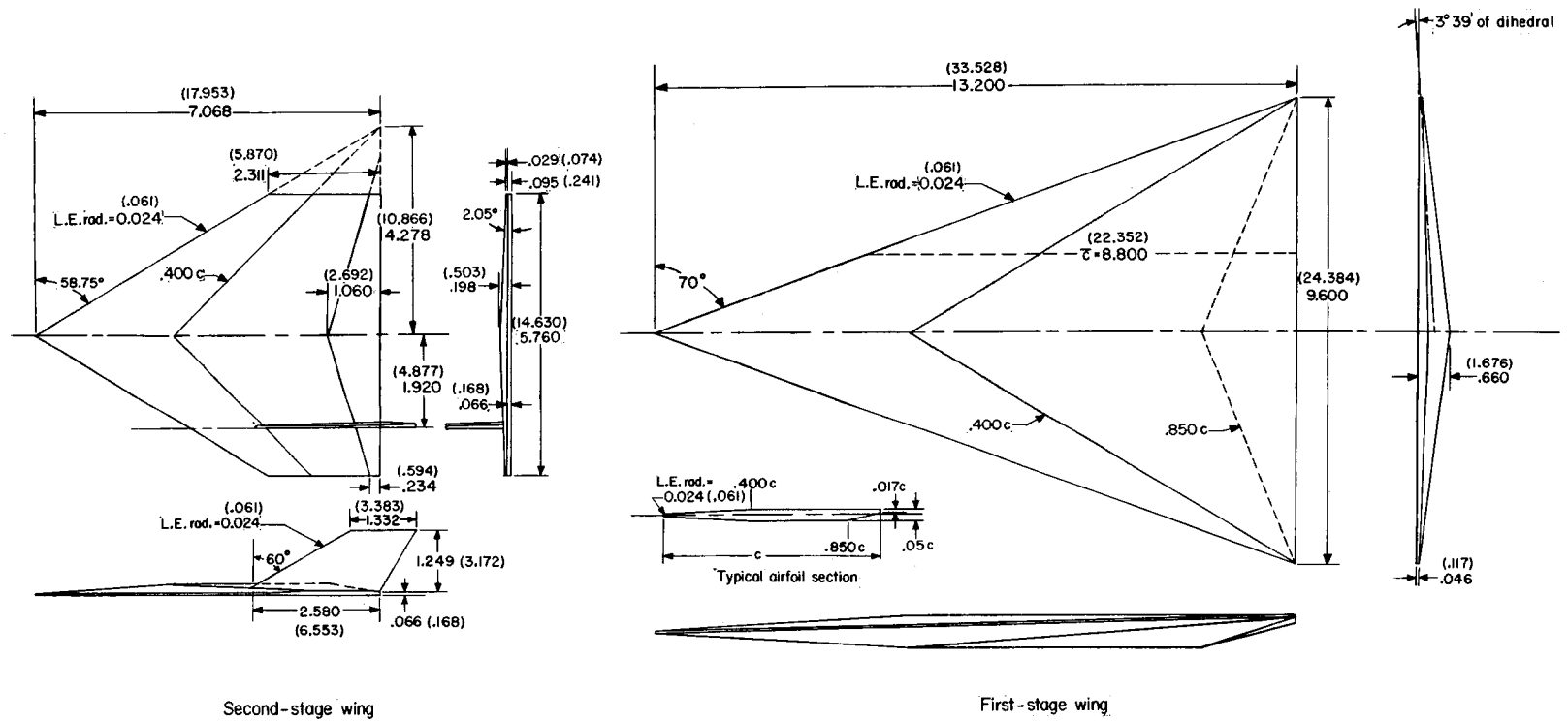

(c) Details of first-stage wing and second-stage wing and fins.

Figure 1.- Continued.

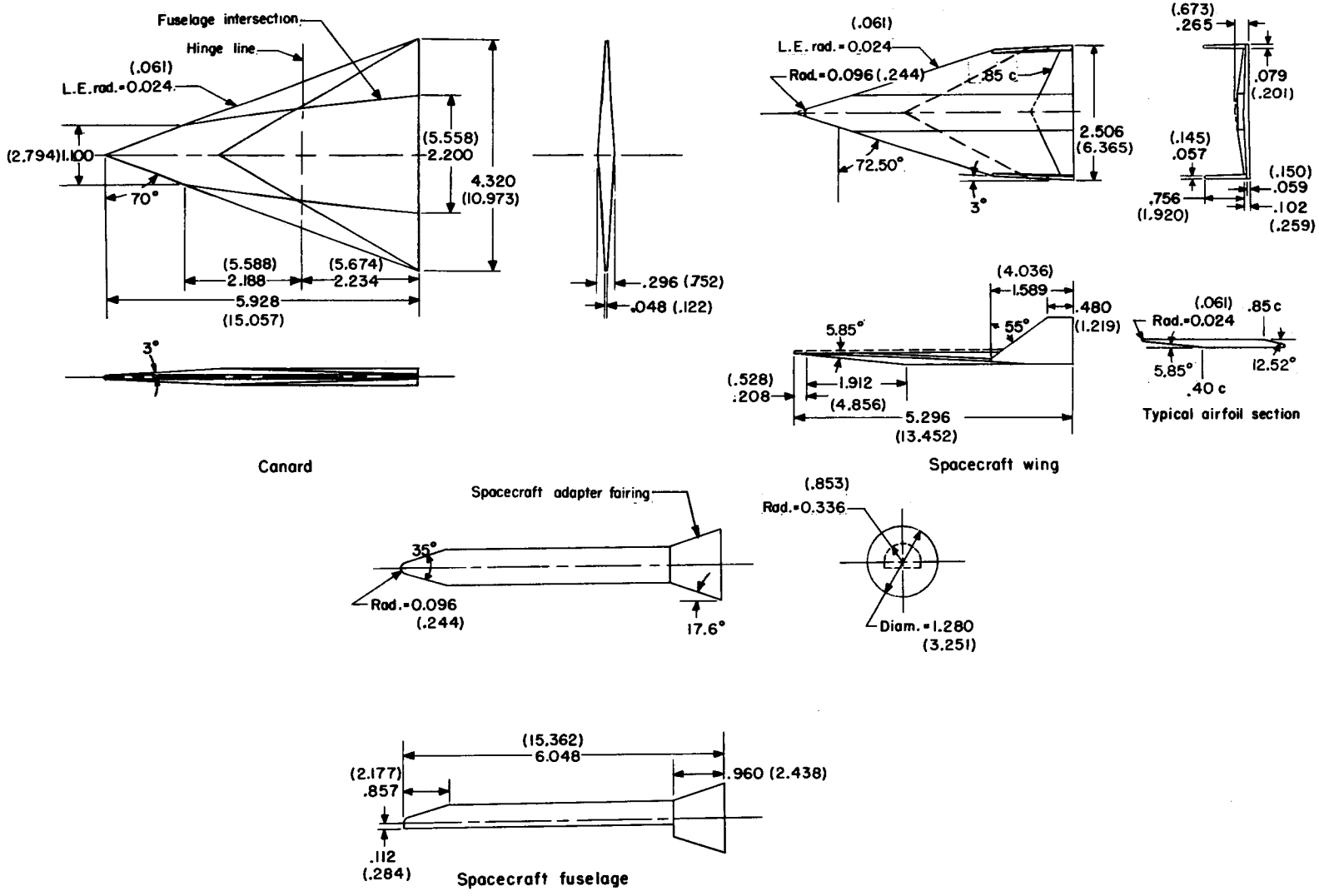

(d) Details of canard and spacecraft.

Figure 1.- Concluded.

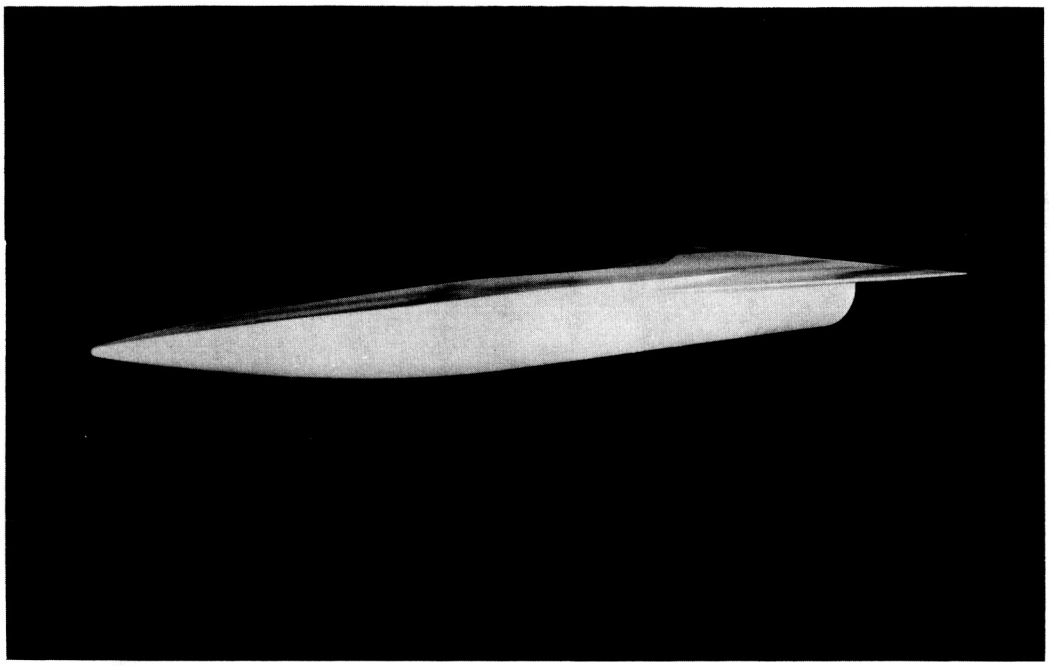

(a) First-stage wing-fuselage combination. L-63-6494

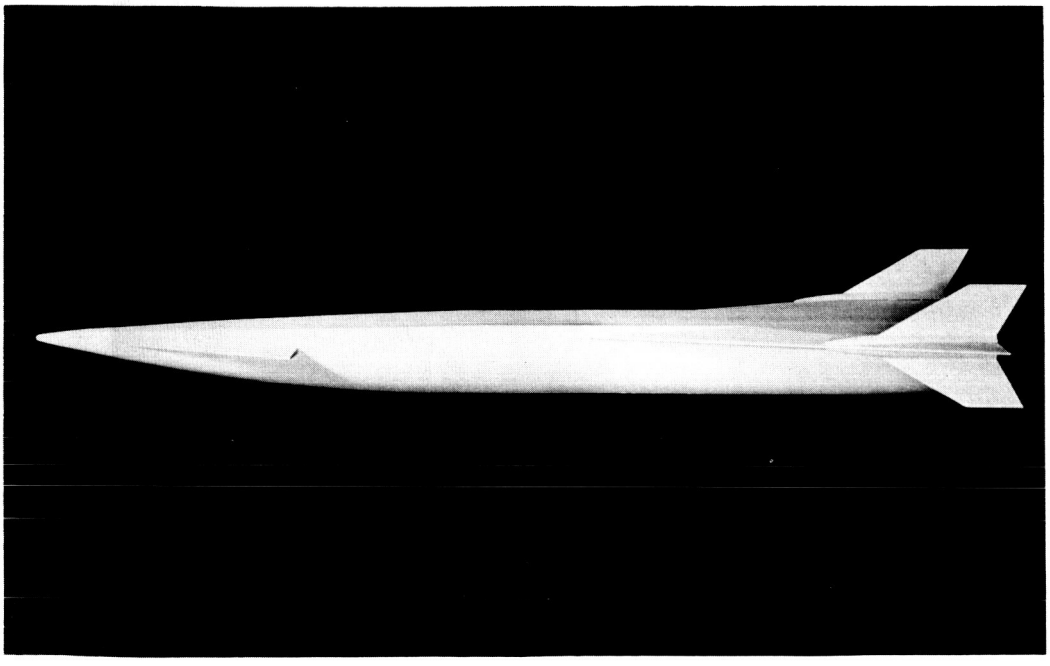

(b) Complete first-stage reusable booster. L-63-6483

Figure 2.- Photographs of model configurations.

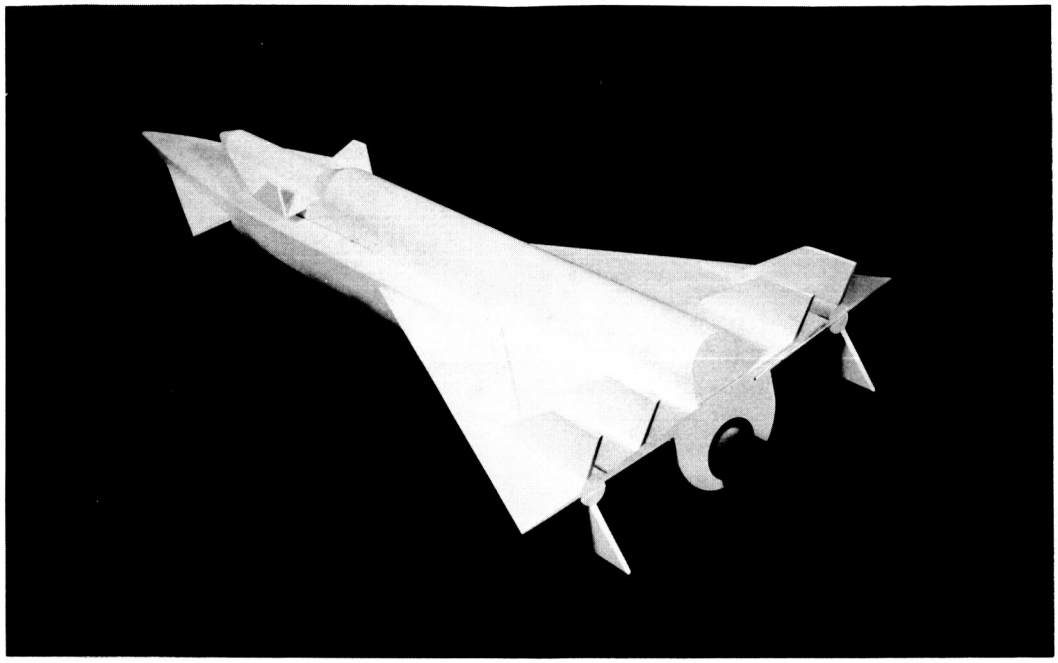

(c) Complete launch vehicle. L-63-6489

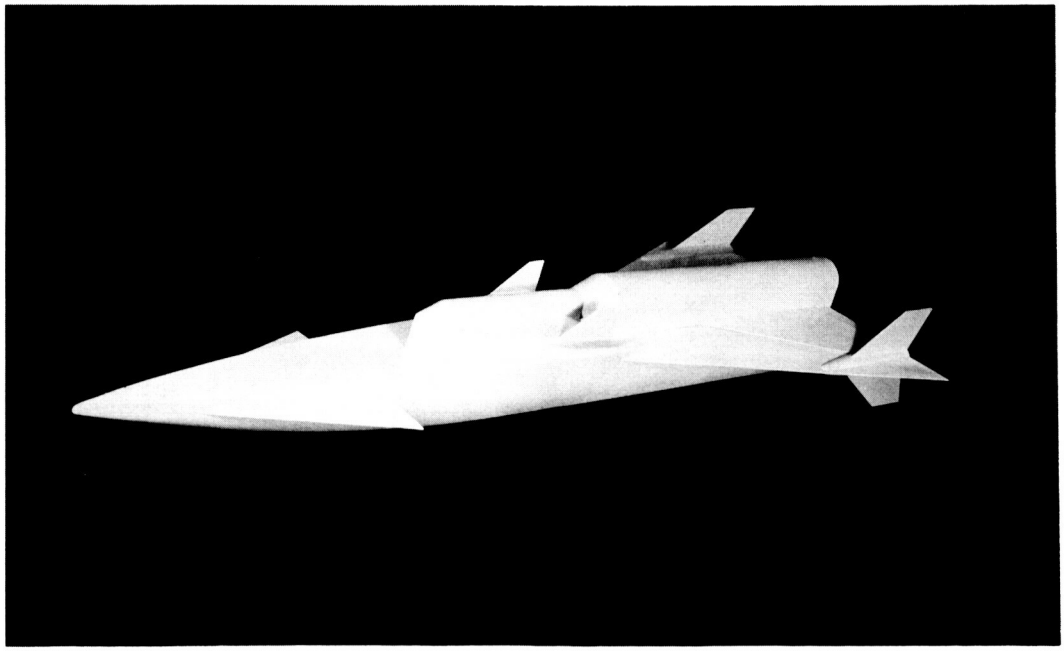

(d) Launch vehicle without maneuver propulsion package. L-63-6481

Figure 2.- Concluded.

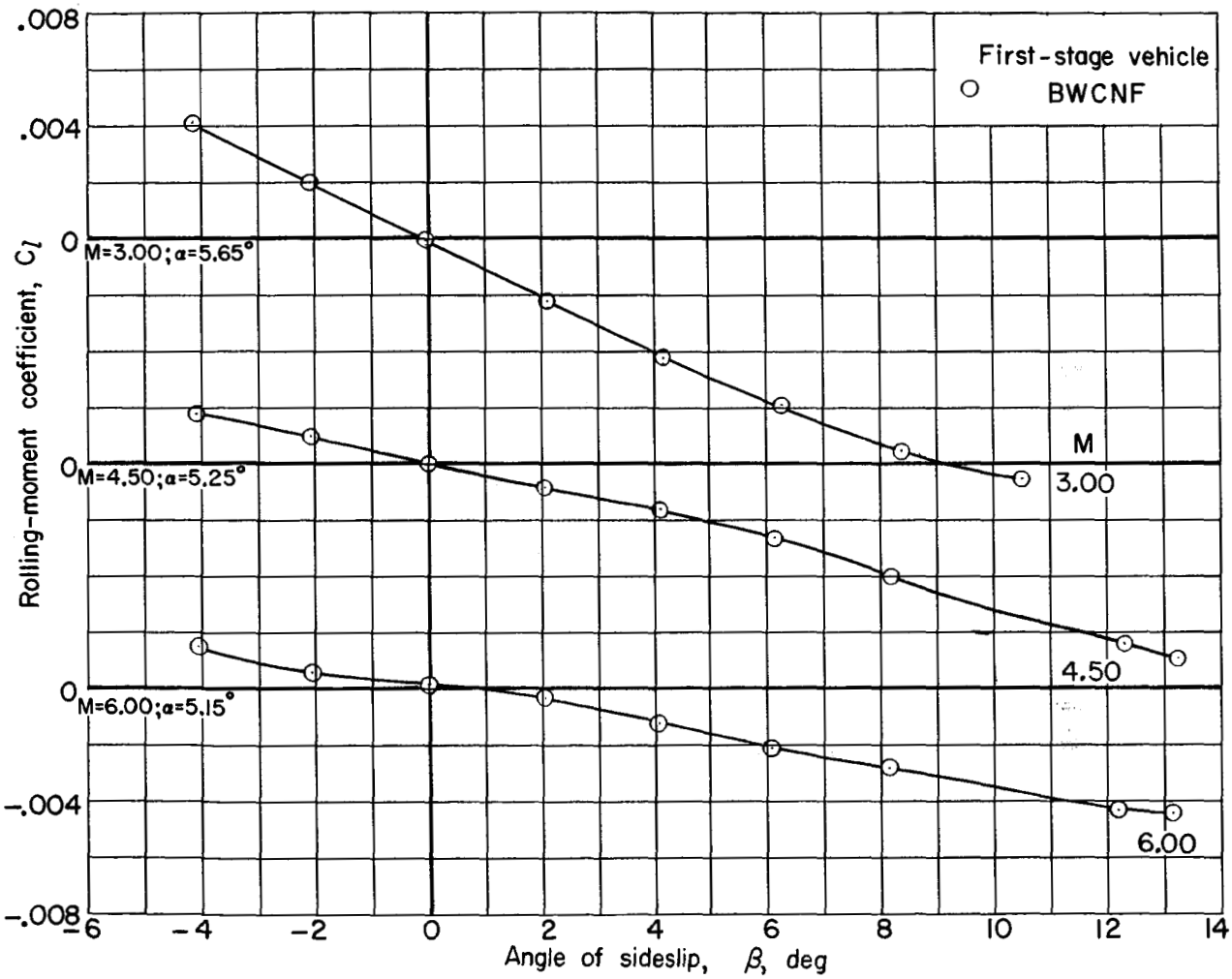

(a) Variation of rolling-moment coefficient with angle of sideslip.

Figure 3.- Lateral aerodynamic characteristics for complete first stage.

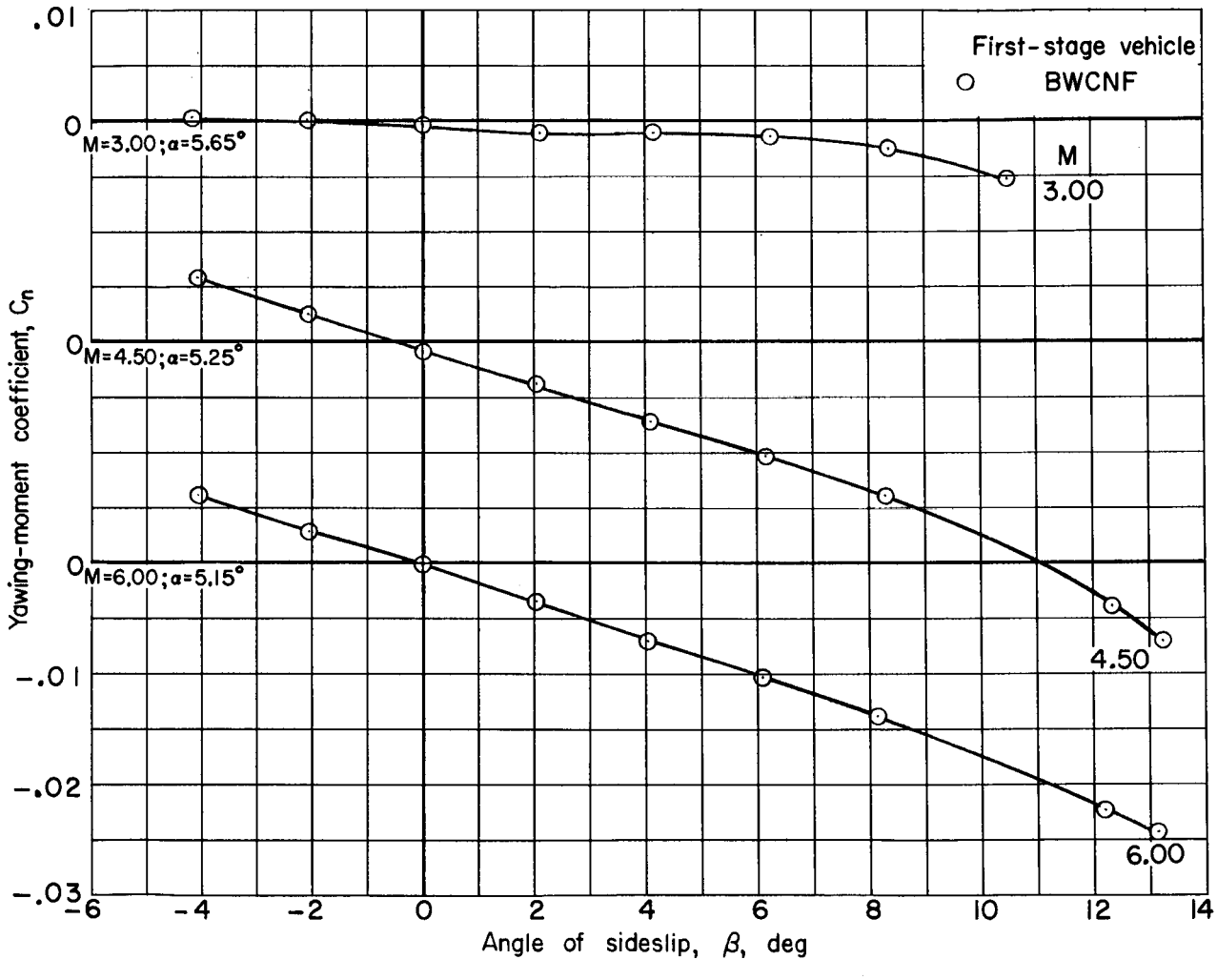

(b) Variation of yawing-moment coefficient with angle of sideslip.

Figure 3.- Continued.

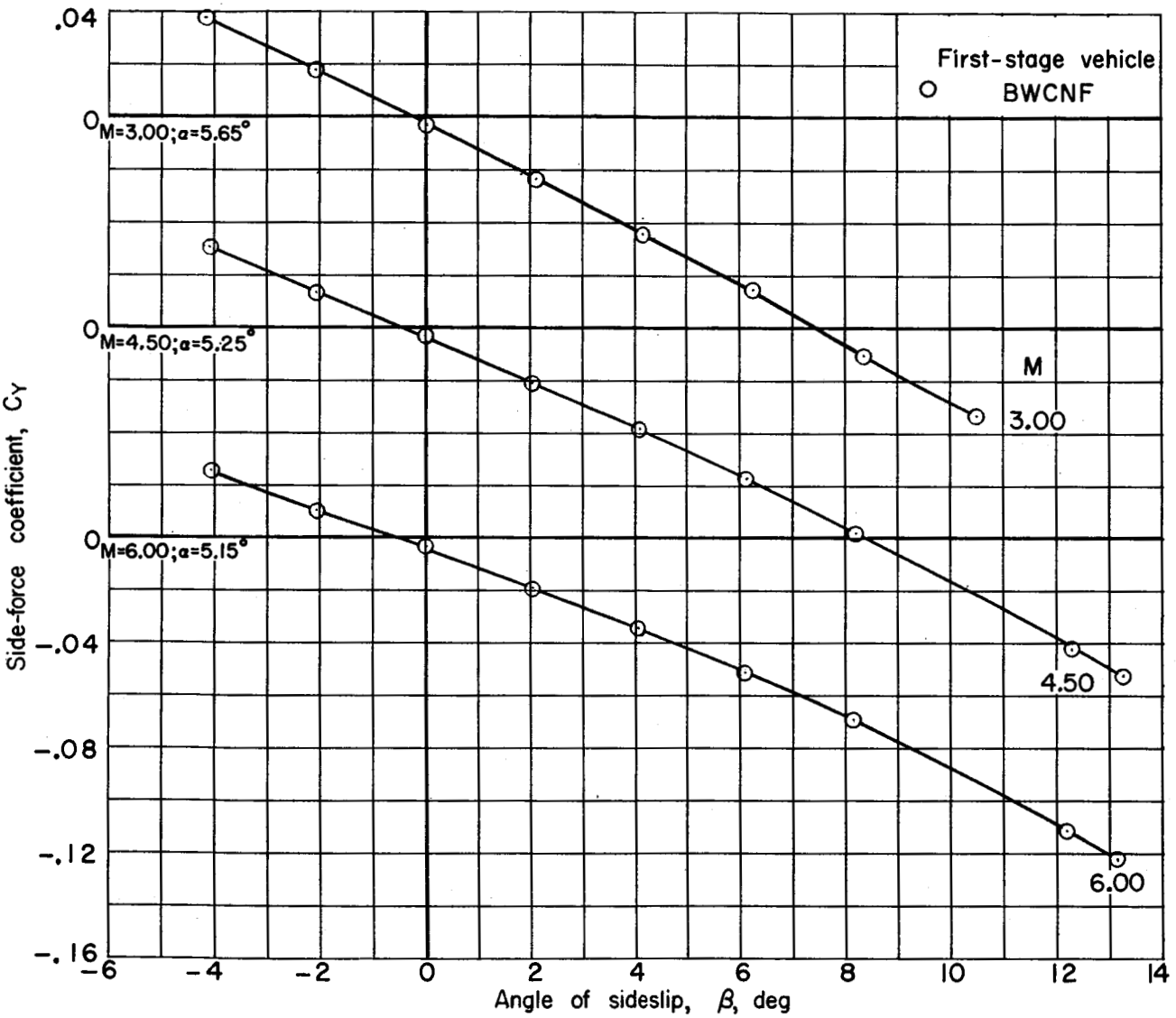

(c) Variation of side-force coefficient with angle of sideslip.

Figure 3.- Concluded.

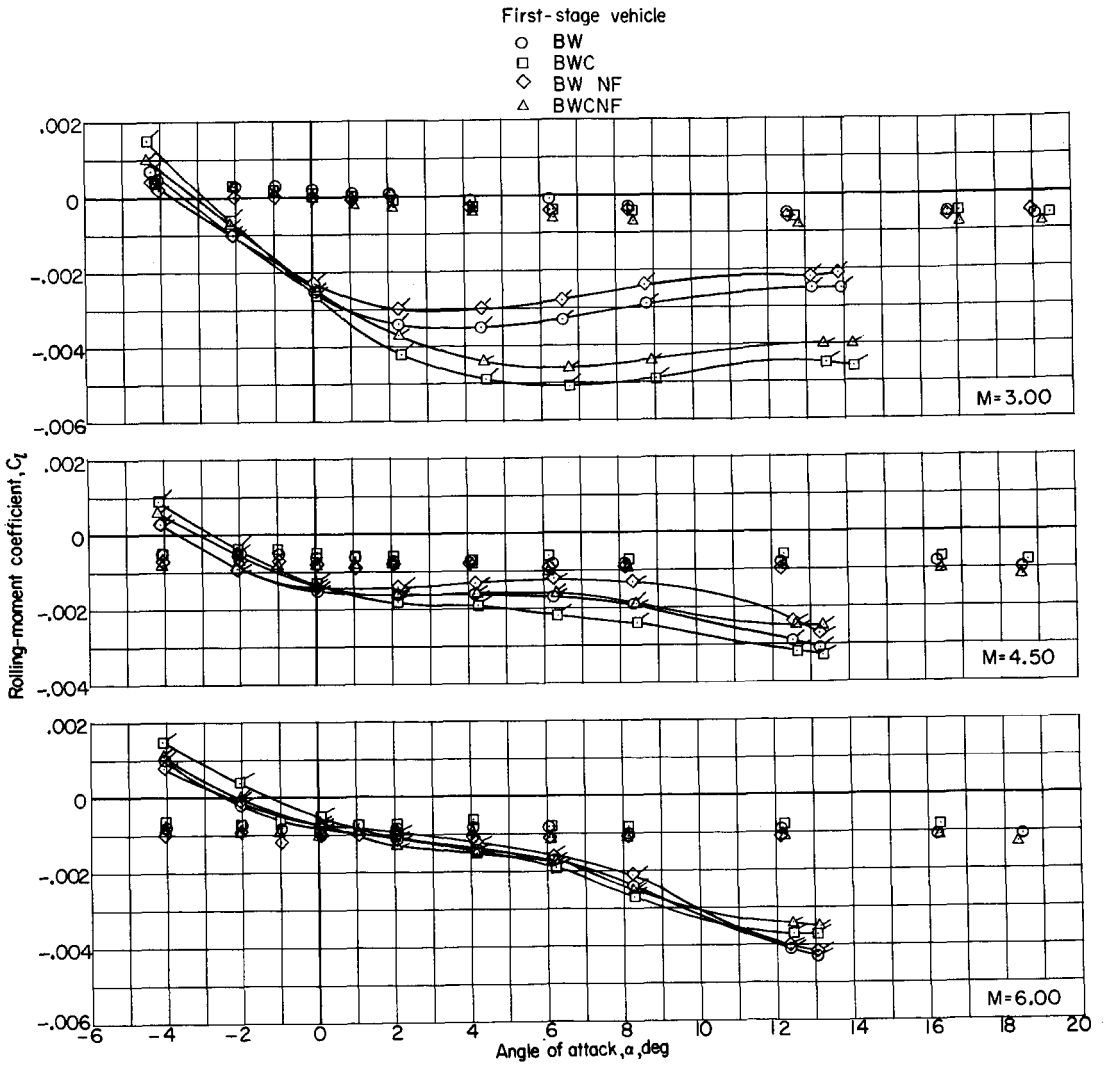

(a) Variation of rolling-moment coefficient with angle of attack.

Figure 4.- Lateral aerodynamic characteristics for several first-stage configurations. $\beta \approx 0^\circ$ and 5°. (Flagged symbols refer to $\beta \approx 5^\circ$.)

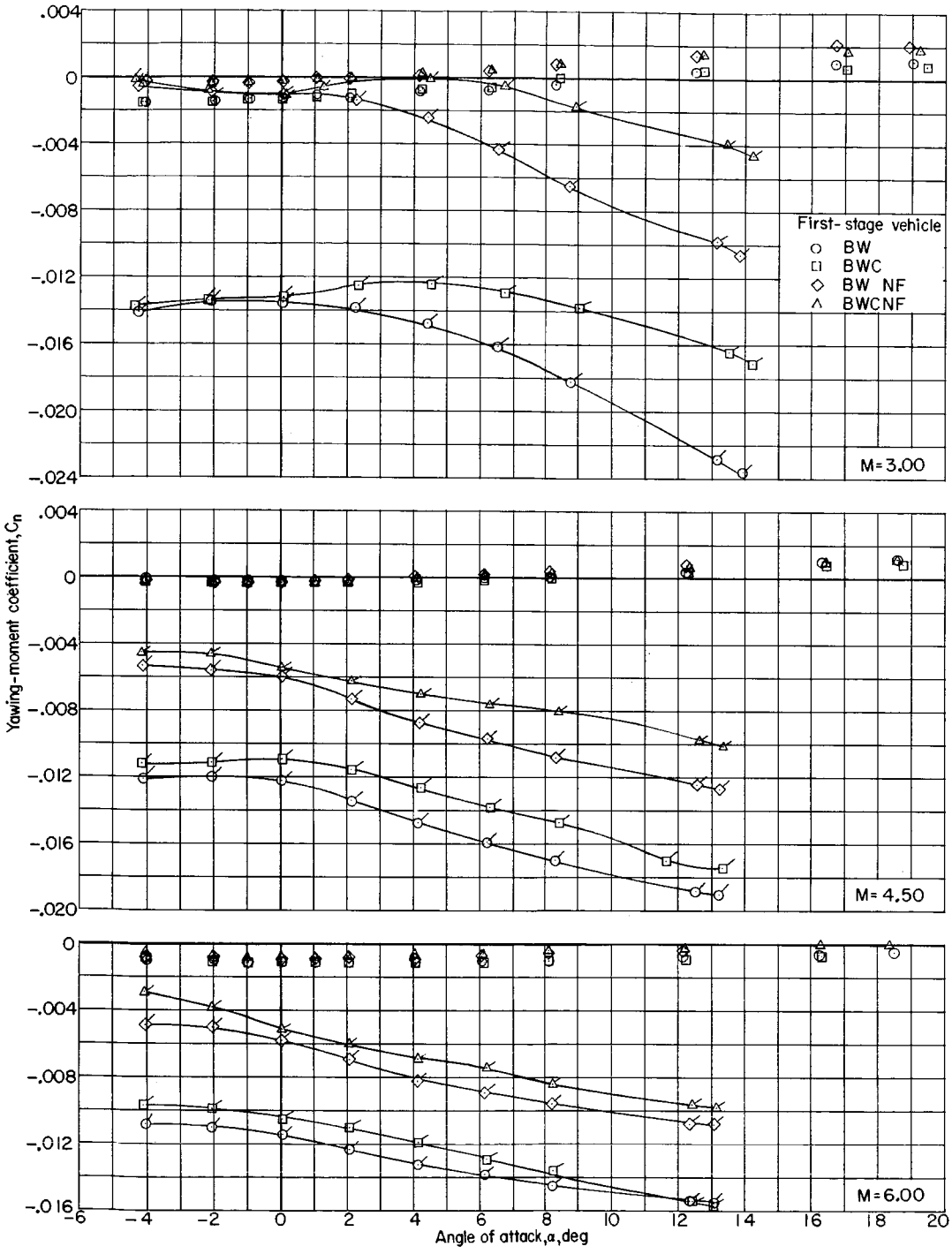

(b) Variation of yawing-moment coefficient with angle of attack.

Figure 4.- Continued.

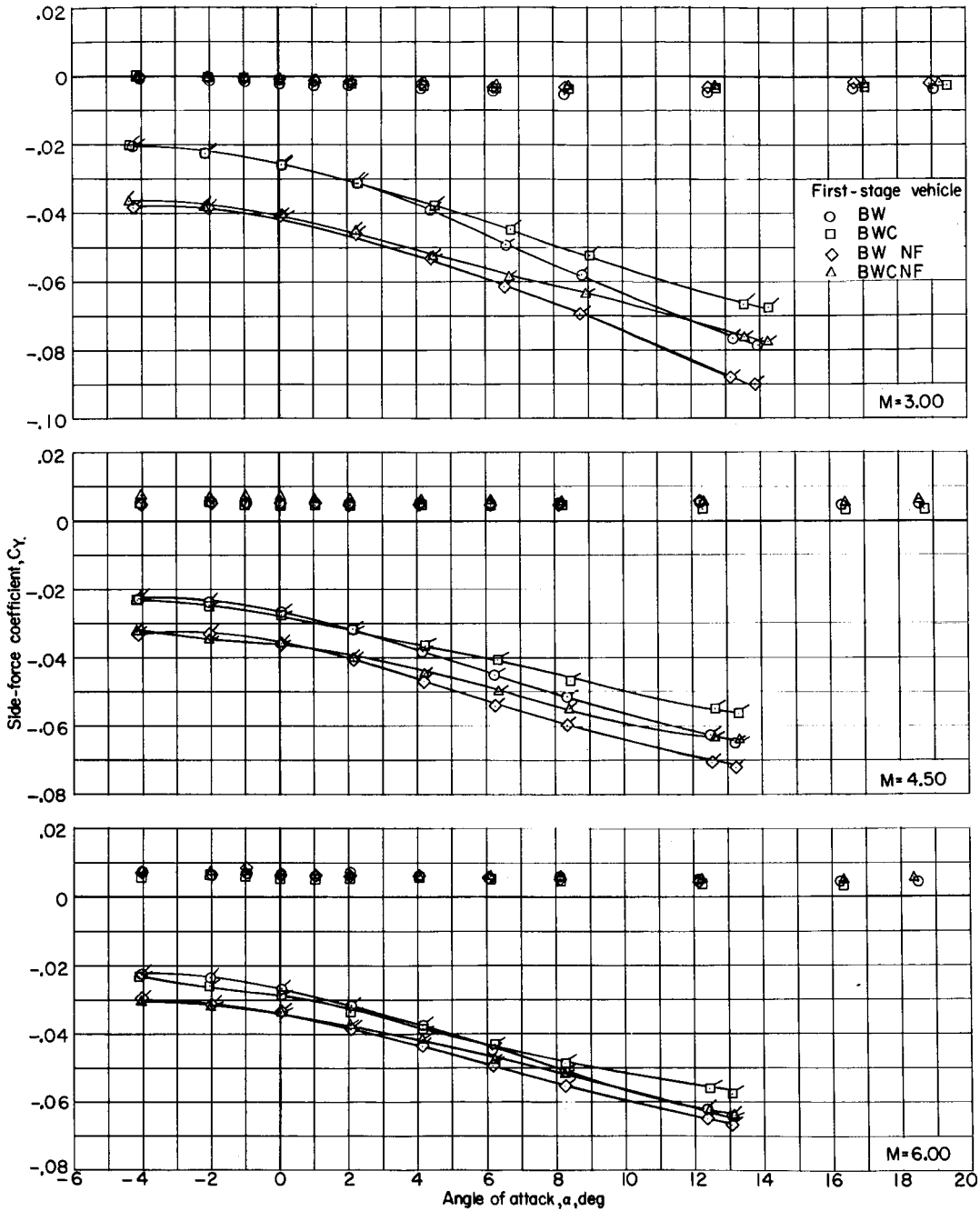

(c) Variation of side-force coefficient with angle of attack.

Figure 4.- Concluded.

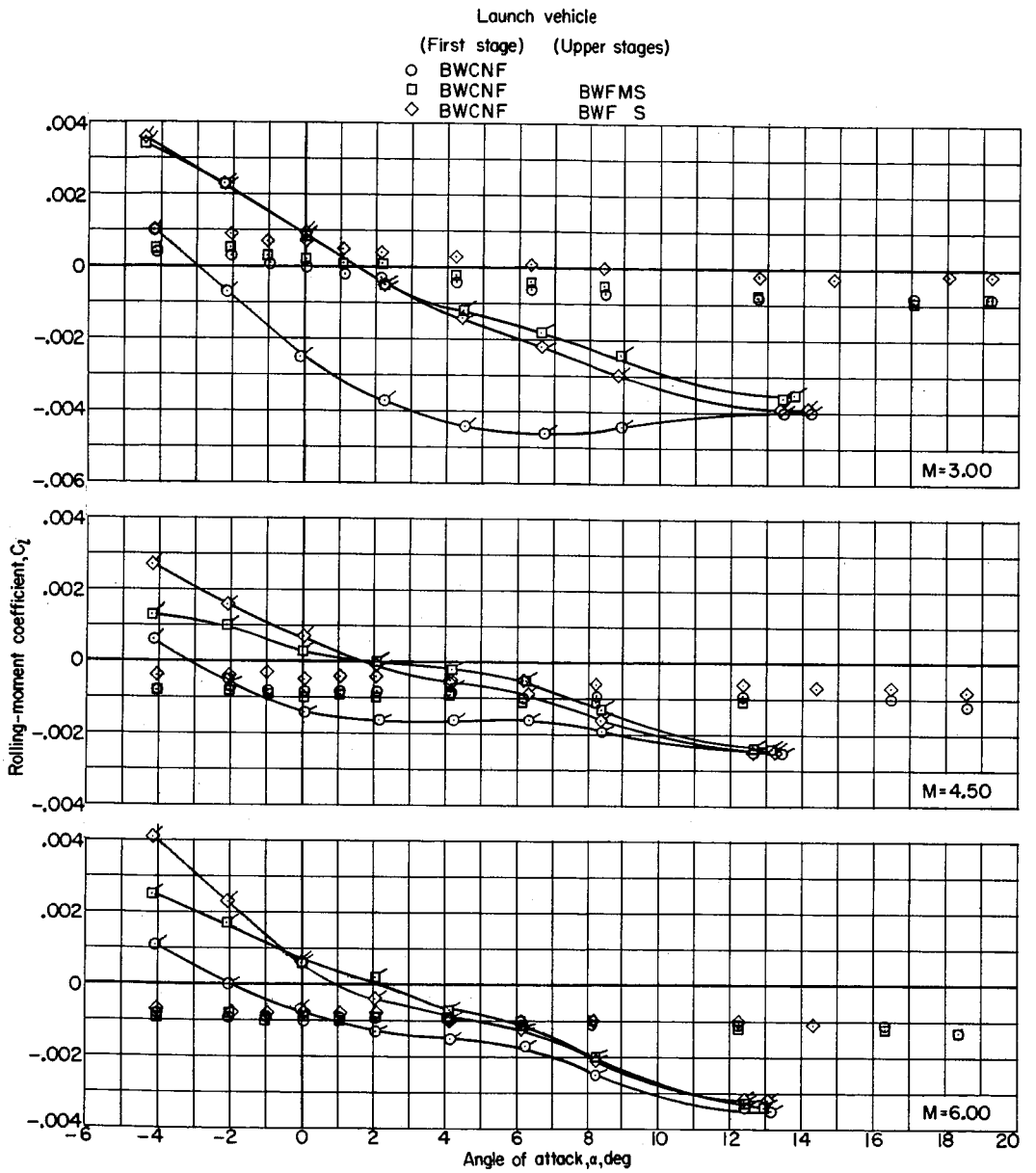

(a) Variation of rolling-moment coefficient with angle of attack.

Figure 5.- Lateral aerodynamic characteristics for several launch-vehicle configurations. $\beta \approx 0^\circ$ and 5°. (Flagged symbols refer to $\beta \approx 5^\circ$.)

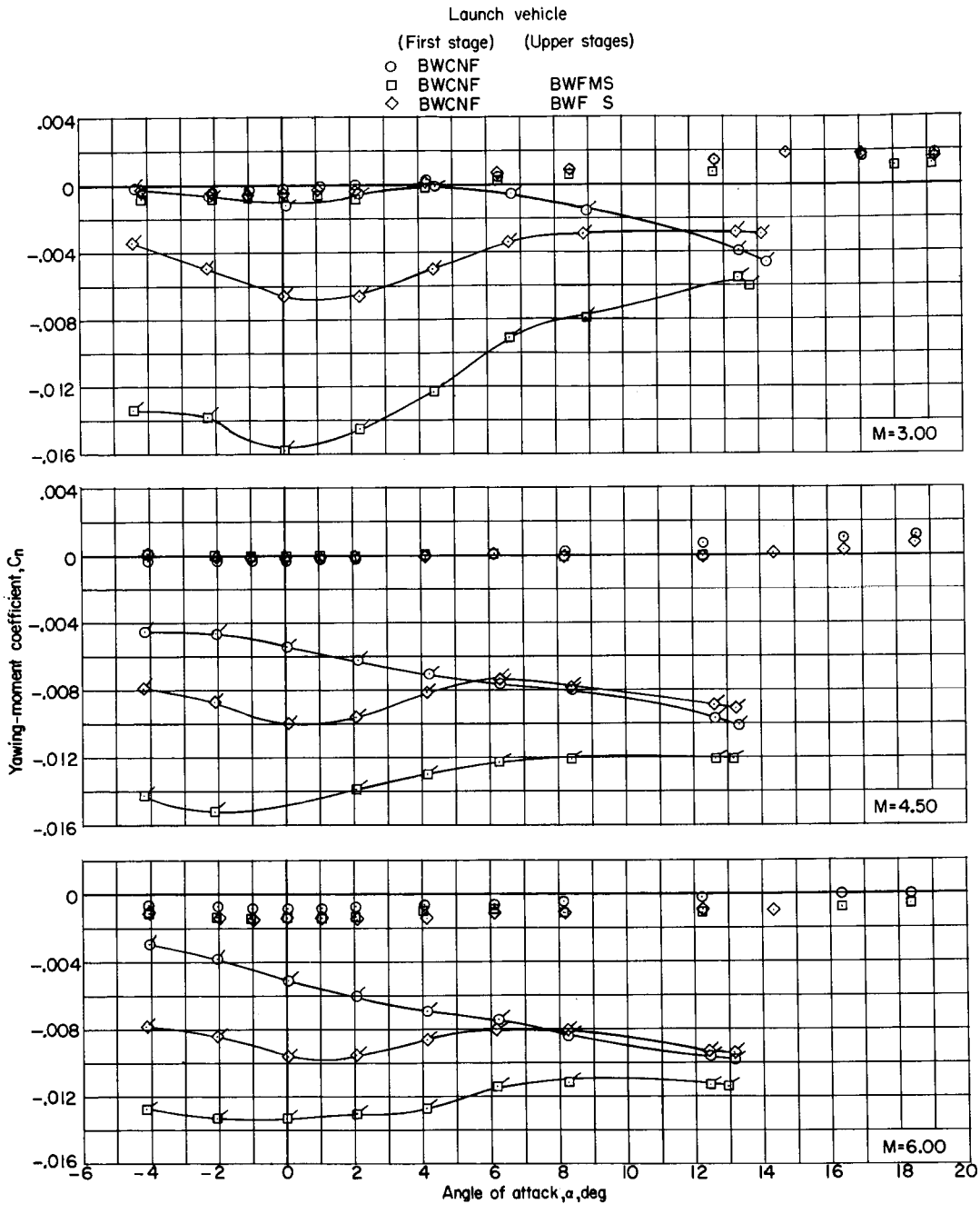

(b) Variation of yawing-moment coefficient with angle of attack.

Figure 5.- Continued.

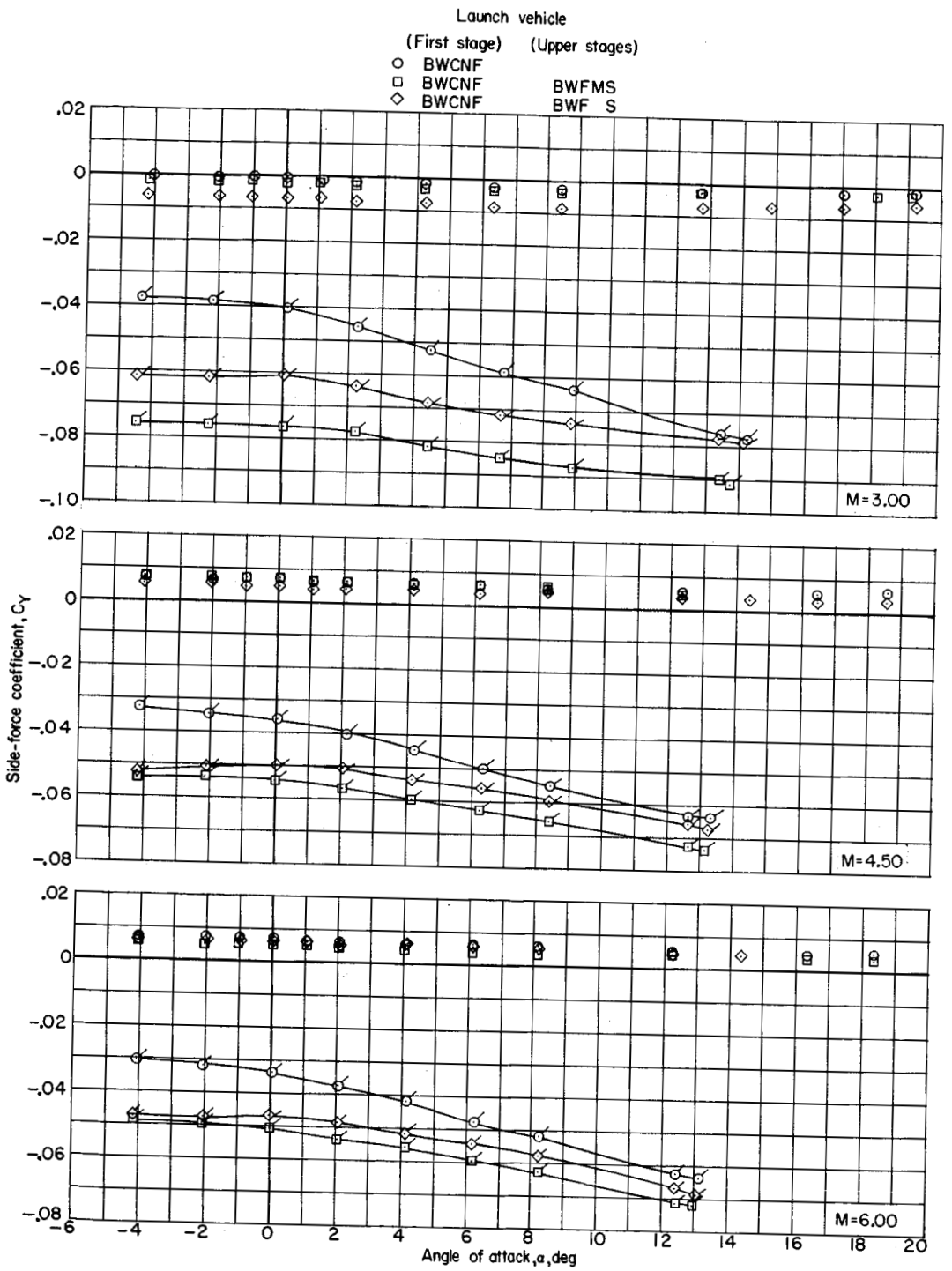

(c) Variation of side-force coefficient with angle of attack.

Figure 5.- Concluded.

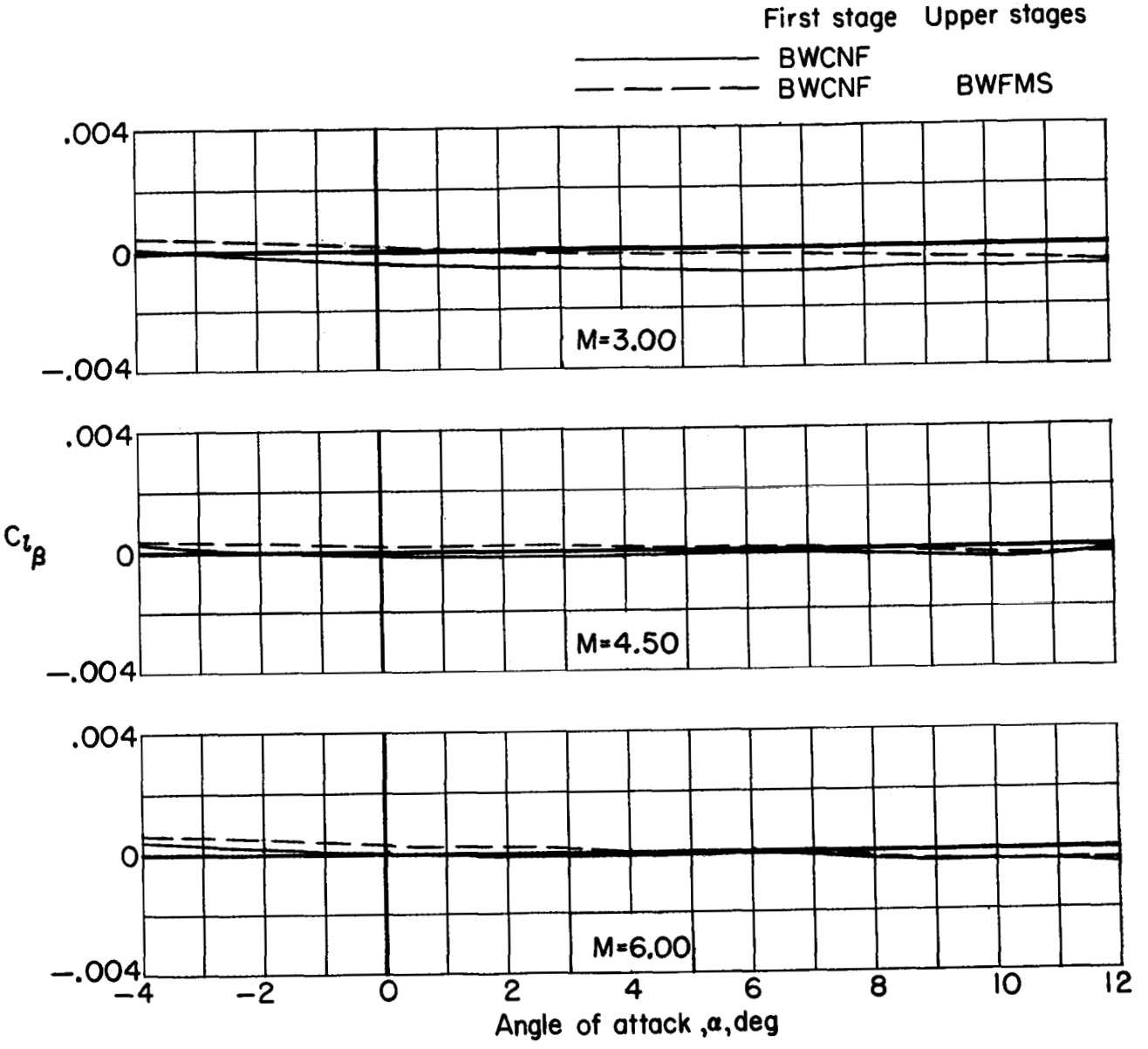

(a) Variation of lateral-stability parameter with angle of attack.

Figure 6.- Variation with angle of attack of lateral- and directional-stability and side-force parameters for complete first stage and complete launch vehicle.

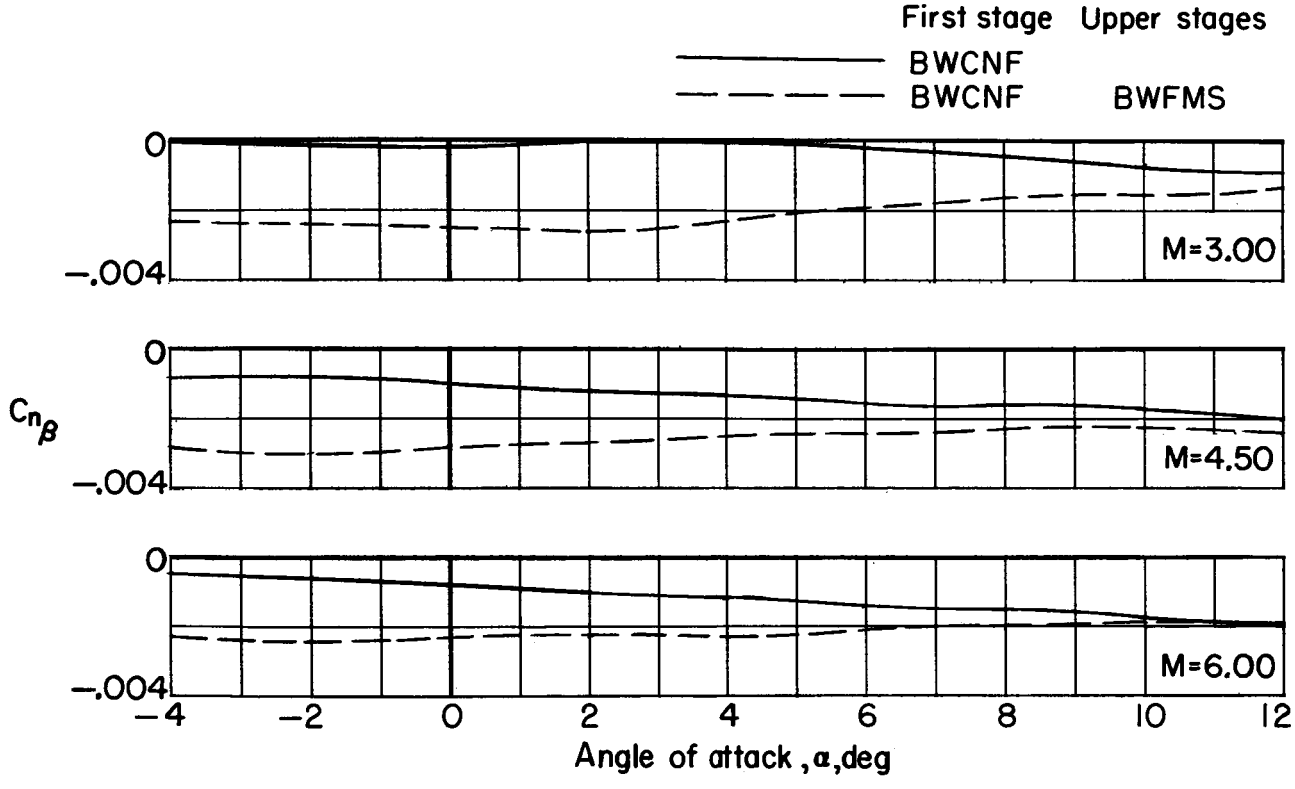

(b) Variation of directional-stability parameter with angle of attack.

Figure 6.- Continued.

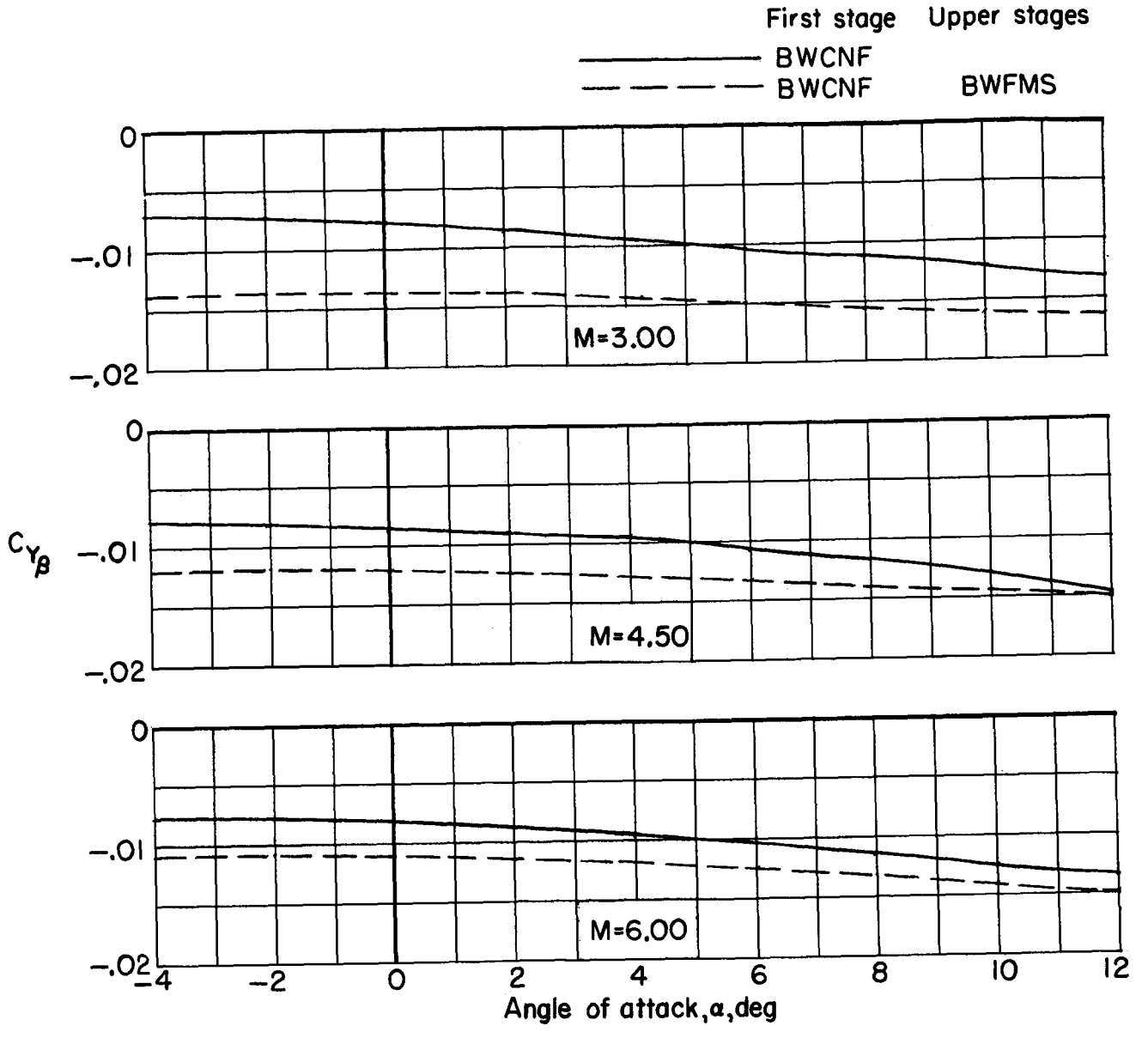

(c) Variation of side-force parameter with angle of attack.

Figure 6.- Concluded.

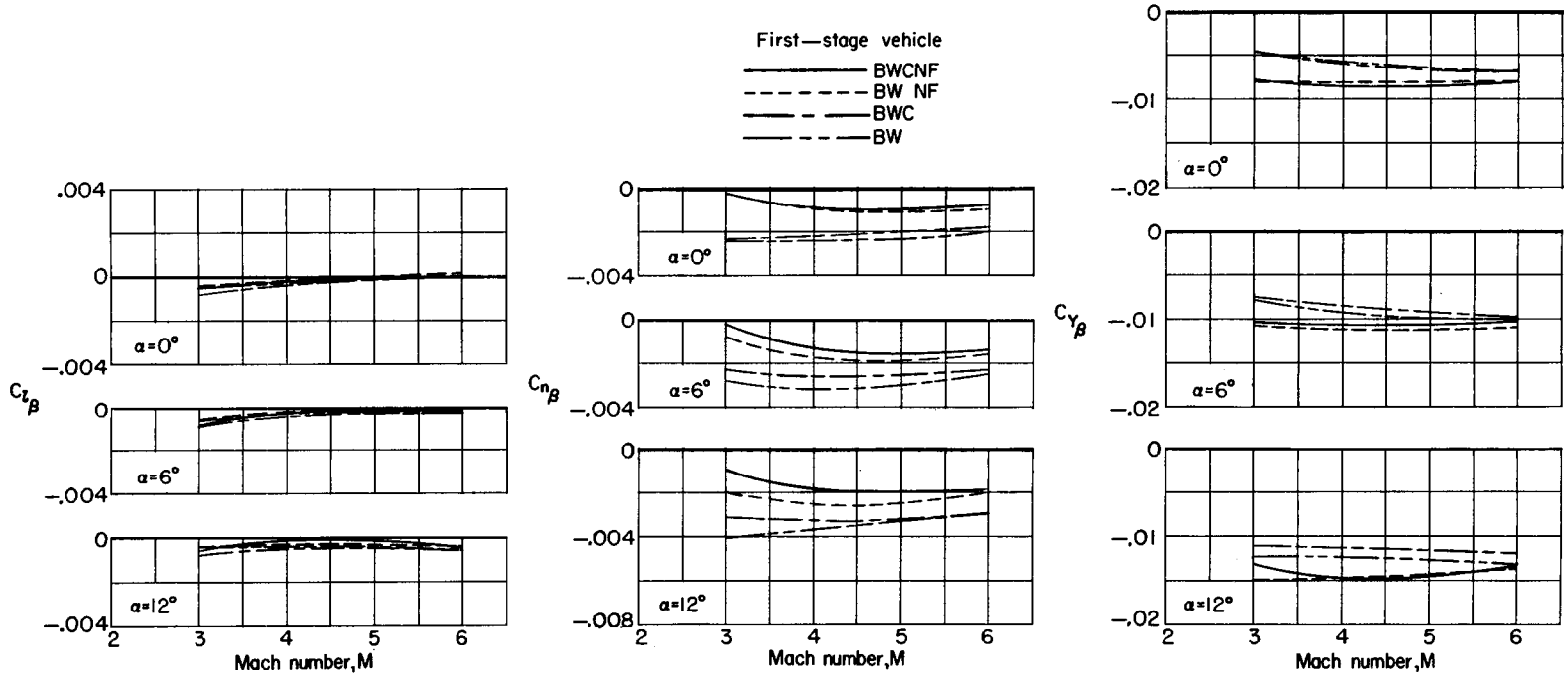

Figure 7.- Variation with Mach number of lateral- and directional-stability and side-force parameters for several first-stage configurations. $\alpha = 0^\circ$, 6°, and 12°.

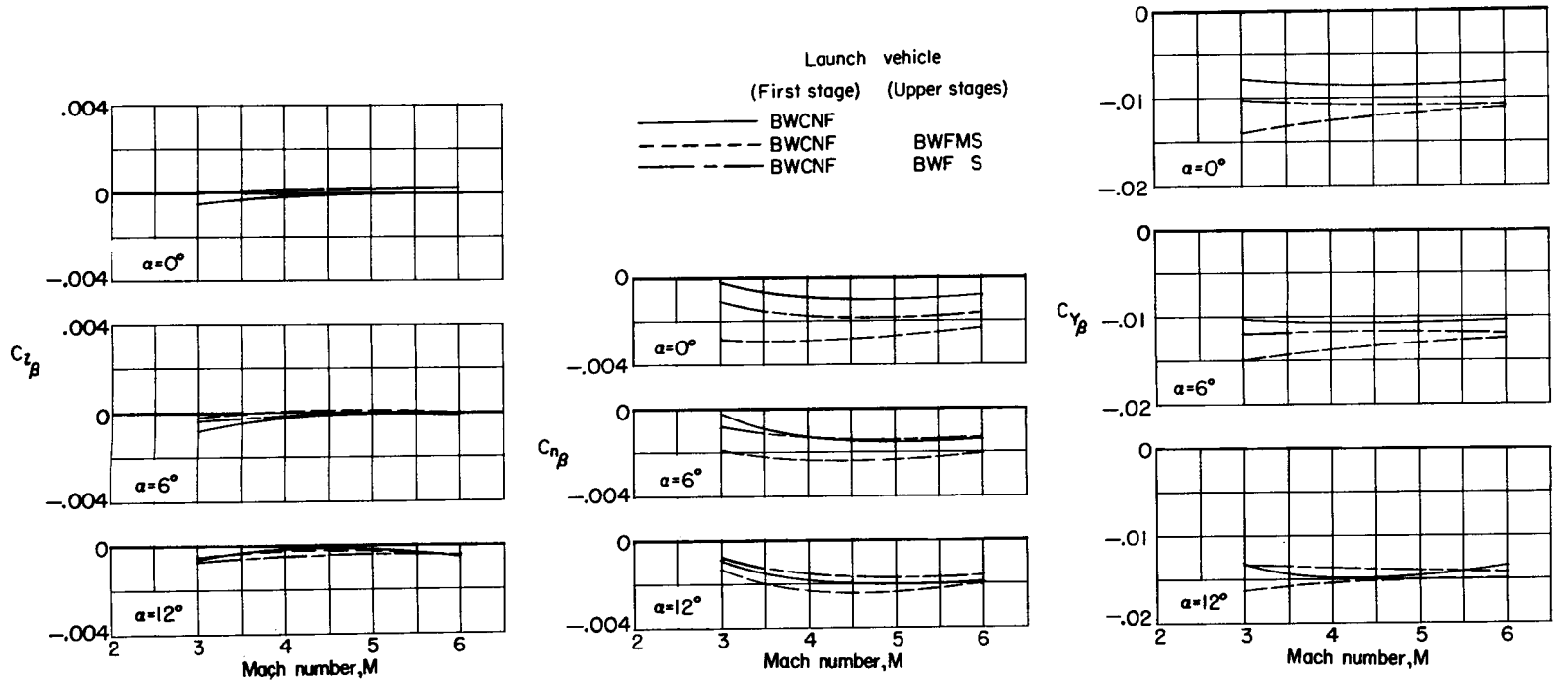

Figure 8.- Variation with Mach number of lateral- and directional-stability and side-force parameters for several launch vehicle configurations. $\alpha = 0^\circ$, 6°, and 12°.